

# Monthly Report (Yamamoto Lab.)

date: 2018.Jun.30  
 Author: R. Oechslin (M2)

Research theme: **Haptic Feedback Controller with Palm Pressurization**

## — Research Plan —

Term \ Month	2	3	4	5	6	7	8	9	10	11	12	1
Literature review												
Design PlayStation Controller												
Test PlayStation Controller												
Frequency Response Analysis												
Design Pilot Controller												
Test Pilot Controller												
Theoretical Analysis												
Analyze data and compare												
Write Thesis												

## — Work Contents —

### 1 Introduction

This report is the continuation of the first two reports about the project "Haptic Feedback Controller with Palm Pressurization". The last report has left off ...

### 2 Theoretical analysis

To come up with a theoretical analysis of the transfer function, a simplifying mechanical schematic has been drawn. This schematic can be seen in figure 1. The equations of motion

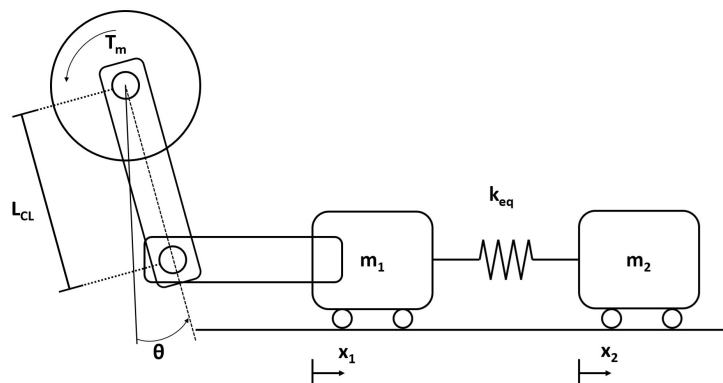


Figure 1: Simplifying mechanical schematic of the actuation system with the stimulator.

can be formulated with the major parameters defined in the schematic. A full explanation of all parameters can be seen in table ???. The variables with subscript 1 refer to the first mass element, the carriage in its guideway, whereas variables with subscript 2 refer to the stimulator, the palm

pad. For the motor the subscript  $m$  has been used.

### Assumptions

First of all, it is important to mention that the transfer function is non-linear, due to the motor angle  $\theta_m$  that determines the force acting on the carriage  $c_1$ . As an initial approach however, this effect has been neglected. More specifically, it is assumed that  $\theta \ll 1$  and  $\cos(\theta) \frac{T_m}{L_{CL}} = F_{carr}$  becomes  $\frac{T_m}{L_{CL}} \simeq F_{carr}$ . Here the angle  $\theta$  is the angle of the lever, pushing the carriage (ie.  $\theta_m = n\theta$ ). Furthermore, there are several types of friction in the system: the intrinsic friction within the motor and its reduction gear, inside the bearings and the carriage in its guideway. Additionally the springs have a non-negligible damping coefficient. In this work the overall friction and the spring damping have been merged and are represented by the friction coefficient  $b_{sp}$ . The stimulator also called the palm pad, is not in contact with the controller, but with the operator. To model the damping of the skin of the operator and the friction between the skin and the palm pad, the damping coefficient  $b_{op}$  has been introduced. Similarly the spring constant of the operator's skin is modeled by  $k_{op}$ .

### Spring Constant and Damping Coefficient of the Operator's Hands

The order of magnitude of the two coefficients  $k_{op}$  and  $b_{op}$  can be found in research papers [Kuchenbecker et al., 2003] [Park et al., 2014] [Speich et al., 2005]. They all indicate parameters varying in the same order of magnitude, namely  $k_{op} \simeq 400\text{N/m}$  and  $b_{op} \simeq 5\text{Ns/m}$ .

### Identification of the Spring Damping Coefficient

The damping coefficient of the spring  $b_{sp}$  can be found by comparing the theoretical results of the frequency response analysis with the experimental findings. In fact, for the experimental setup, the stimulator has been fully blocked and therefore the operators spring coefficient can be seen as infinitely stiff.

By varying  $b_{sp}$  and Bode-plotting the results of the analytical transfer function, the coefficient's order of magnitude can be found. In order to do so, the analytical transfer function has to be identified.

### Expected Transfer Functions

The system can be cut into two major transfer functions. The block diagram including these two transfer functions is depicted in figure 2.

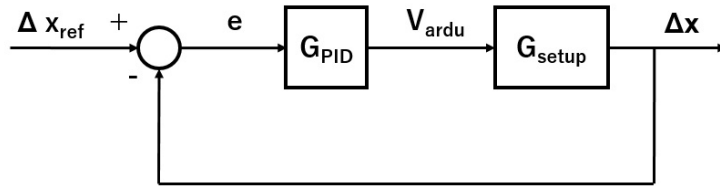


Figure 2: Block diagram with two different transfer functions.

According to this figure one can obtain a transfer function of the following form:

$$F(s) = G_{PID}(s)G_{setup}(s) = \frac{V_{ardu}}{E} \frac{\Delta X}{V_{ardu}} = \frac{\Delta X(s)}{E(s)} \quad (1)$$

where  $V_{ardu}$  is the voltage output of the arduino for controlling the motor. Using this form one can calculate the individual transfer functions and finally relate the compression of the springs  $\Delta x$  to the compression given as reference  $\Delta x_{ref}$ .

**PID Transfer Function** The transfer function given by the PID controller is very straightforward and can be taken out of any control theory book [Dutton et al., 1997]. Specific for this case is the multiplication factor  $K_{PID2Va}$  to get from the PID value to the desired armature voltage level. The transfer function is given in equation 2.

$$G_{PID}(s) = \frac{V_a(s)}{E(s)} = K_{PID2Va}(K_P + \frac{K_I}{s} + K_D s) \quad (2)$$

Finally, there is also the gain of the amplifier in voltage mode, which converts the voltage of the Arduino into the voltage applied to the motors. This gain is  $K_{ampl} = 10\text{Volt/Volt}$ . To this voltage an offset voltage of  $V_{offset} = -20\text{V}$  is added.

**Motor Equations** The second transfer function relates the motor torque  $T_m$  to the Arduino voltage as well as the output  $\Delta x$  to  $T_m$ . Due to the back electromotive force these two parts are related and have to be treated as a whole.

The output torque  $T_m$  of the motor can be calculated using the sums of all torques and the conversion parameters intrinsic to the motor.

Similar to the setup and analysis in [Junior et al., 2016] the equations of the motor are given as:

$$L_a \frac{di_a}{dt} + R_a i_a + K_{emf} \dot{\theta}_m = V_a \quad (3)$$

where  $L_a$  is the armature inductance,  $R_a$  the armature resistance and  $i_a$  the armature current of the motor.  $K_{emf}$  is the back electromotive force constant also given by the motor.  $V_a$  is the armature voltage and  $\theta_m$  is the angle of the motor shaft.

Furthermore, with Newtons law, the sum of all torques must be zero, or:

$$J_T \ddot{\theta}_m - \frac{k_{eq} L_{CL}}{n} \Delta x - \frac{b_{sp} L_{CL}}{n} (\dot{x}_2 - \dot{x}_1) = T_m = K_\tau i_a \quad (4)$$

In equation 4 the parameter  $J_T$  stands for the total equivalent inertia of the motor and the clamping link and  $K_\tau$  is the proportional current torque gain constant. The moment of inertia can either be calculated as the sum of all inertias seen by the motor shaft, or measured in a simple test.

The total inertia of the system is determined by the inertia of the rotor  $J_m$ , the gear inertia  $J_g$ , the inertia of the clamp link  $J_{CL}$  as well as the inertia of the carriage assembly with mass  $m_1$ . The last one can be found by simplifying the load to a point mass at distance of the clamp link length  $L_{CL}$ , which is given by  $J_{carr} = m_1 L_{CL}^2$ . The gear box increases the inertia seen by the motor shaft by the square of its ratio  $n$ :

$$J_{load, motor \ side} = n^2 J_{load} \quad (5)$$

We therefore have a total inertia of:

$$J_T = J_m + J_g + n^2 J_{CL} + n_2^2 m_1 L_{CL}^2 \quad (6)$$

where  $J_{CL}$  can be calculated by approximating it as a cantilever with an off-center axis of distance  $l$ <sup>1</sup>:

$$J_{CL} = \frac{1}{12} m_{CL} (A^2 + B^2 + 12l^2) \quad (7)$$

where  $A$  and  $B$  are the width and length respectively.

The conversion between the angle  $\theta$  and the distance  $x$  can be found by assuming that the horizontal displacement of the carriage is given by  $L_{CL} \sin(\theta) = x$ . For small angles of  $\theta$  the Taylor expansion gives:

$$L_{CL} \theta \simeq x_1 \quad (8)$$

The output  $\Delta x$  is the compression of the springs and is given by  $\Delta x = x_2 - x_1$ . For finding  $x_2$  the equation of motion given by Newtons law has to be considered.

$$m_2 \ddot{x}_2 = -k_{eq}(x_2 - x_1) - b_{sp}(\dot{x}_2 - \dot{x}_1) - k_{op}x_2 - b_{op}\dot{x}_2 \quad (9)$$

In the case where the stimulator has been blocked,  $x_2$  has been forced to zero. Using the Laplace transform and equation 9 one finds the expression of  $x_2$ :

$$X_2 = -\frac{k_{eq} + b_{sp}s}{s^2 m_2 + b_{op}s + k_{op}} \Delta X \quad (10)$$

**Motor and Spring Transfer Function** Combining all the equations one can find the final block diagram, which can be seen in figure 3

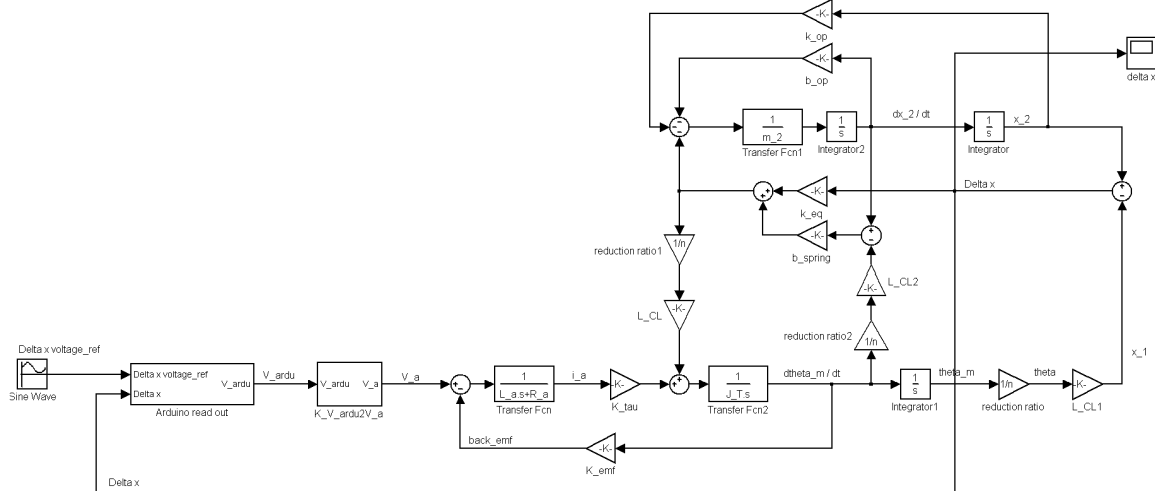


Figure 3: Complete block diagram relating the output  $\Delta x$  to the input  $\Delta x_{ref}$ .

From this diagram and the equations mentioned above, one can obtain the transfer functions that relate the output  $\Delta x$  and input  $\Delta x_{ref}$  as introduced in equation 1, where  $\Delta X(s)$  and  $\Delta X_{ref}(s)$

<sup>1</sup>(2018, June 19th) retrieved from <http://www.orientalmotor.com/technology/motor-sizing-calculations.html>

are the Laplace transforms of the output and input functions respectively.

It is thus possible to study the frequency response by simulating this setup with the assumptions mentioned earlier.

### Main Equations for Analytical Transfer Function

$$\Delta X_{ref} - \Delta X = E \quad (11)$$

$$(K_P + K_D s + \frac{K_I}{s}) E K_{PID2} V_a = V_a \quad (12)$$

$$\frac{V_a - K_{emf} \dot{\theta}_m}{L_a s + R_a} K_\tau + F_{coupled} = J_T \ddot{\theta}_m \quad (13)$$

$$F_{coupled} = (k_{eq} + b_{sp} s) \frac{L_{CL}}{n} \Delta X \quad (14)$$

$$\theta_m = \frac{n}{L_{CL}} X_1 = -\frac{n}{L_{CL}} (1 + \frac{k_{eq} + b_{sp} s}{m_2 s^2 + b_{op} s + k_{op}}) \Delta X \quad (15)$$

In the case of the experimental setup the palm pad has been blocked and therefore  $x_2$  has been forced to be constant. The last equation becomes thus:  $\theta_m = -\frac{n}{L_{CL}} \Delta X$ .

### Analytical Transfer Function

The analytical transfer function has only been calculated for a specific set of spring damping coefficients  $b_{sp}$ . The simulation result that was closest to the experimental setup can be seen in figure 4 and the corresponding transfer function is:

$$\frac{\Delta X}{\Delta X_{ref}} = \frac{7.04 \times 10^{-3} s^2 + 288 s + 2.94 \times 10^6}{1.09 \times 10^{-10} s^5 + 6.69 \times 10^{-6} s^4 + 0.137 s^3 + 940 s^2 + 6.45 s + 2.95 \times 10^6} \quad (16)$$

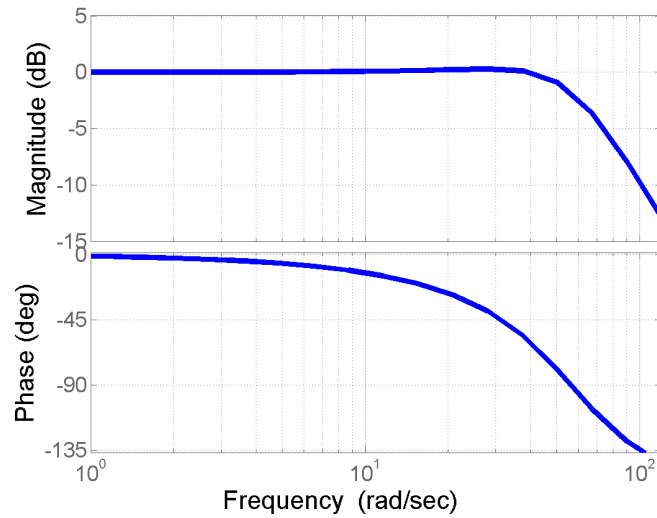


Figure 4: Bode plot of analytical transfer function for  $b_{sp} = 215\text{Ns/m}$ .

As it can be seen in figure 4 there is a constant gain of 1 for lower frequencies and a slight resonance top becomes visible around 166Hz. The phase shift is of around  $140^\circ$  for the frequencies

of interest. Due to the setup constraints, the analytical results of higher frequencies have not been considered.

### **3 Discussion**

asdfdf

### **4 Conclusion**

asdf

### **5 Outlook**

faaafaa adsf

## References

- [Dutton et al., 1997] Dutton, K., Thompson, S., and Barraclough, B. (1997). *The art of control engineering*. Addison Wesley Harlow.
- [Junior et al., 2016] Junior, A. G. L., de Andrade, R. M., and Bento Filho, A. (2016). Series elastic actuator: Design, analysis and comparison. In *Recent Advances in Robotic Systems*. InTech.
- [Kuchenbecker et al., 2003] Kuchenbecker, K. J., Park, J. G., and Niemeyer, G. (2003). Characterizing the human wrist for improved haptic interaction. In *ASME 2003 International Mechanical Engineering Congress and Exposition*, pages 591–598. American Society of Mechanical Engineers.
- [Park et al., 2014] Park, J., Pažin, N., Friedman, J., Zatsiorsky, V. M., and Latash, M. L. (2014). Mechanical properties of the human hand digits: Age-related differences. *Clinical Biomechanics*, 29(2):129–137.
- [Speich et al., 2005] Speich, J. E., Shao, L., and Goldfarb, M. (2005). Modeling the human hand as it interacts with a telemanipulation system. *Mechatronics*, 15(9):1127–1142.